# NUMERICAL MODELLING OF MORPHODYNAMICS AROUND A TIDAL INLET

Ming Li[1], John Nicholson[1*], Shunqi Pan[2] and Brian A O'Connor[1]

A two-dimensional morphological model is used to study sediment transport and morphdynamics around a tidal inlet. The model includes the processes of erosion on side slope for the avalanching effects. The model has been tested against a laboratory study of an idealised tidal inlet configuration over 68 tidal cycles. The results show a reasonable agreement between the model and experiment measurements with a typical pattern of accretion at up-drift of the inlet and erosion at the down-drift. This study also reveals the importance of surface waves and cross-shore sediment transport to the evolution and migration of the tidal inlet.

Keywords: sediment transport; morphology; tide; numerical model; tidal inlet

## INTRODUCTION

Due to the considerable economic and ecological importance, long term sustainable development of a tidal inlet and the adjacent lagoon has been recognised worldwide in recent years. For example, maintaining the navigation channel and stability of the shoreline position is fundamental to the coastal management scenarios. The water quality within the lagoon is also critical to the dynamic coastal ecosystems. In the face of rising sea level and climate change, the challenge for these complex engineering issues has been significantly amplified. The need for improved engineering models has therefore become crucial for a better understanding of the underlying mechanism and more reliable predictions tools for potential future morphological changes.

Affected by the combined action of waves and tides, the morphodynamics around a tidal inlet is often highly dynamic and complex. To a large extent, its behaviour is determined by the relative contribution of these two forcing factors. In the past, the calculation of long term morphological change in particular often relies on empirical relations, for example, those produced by Bruun *et al*. (1978), Hayes (1979, 1980) and Davis and Barnard (2003). In recent years, the process-based models have been used successfully in tidal dominant environment for simulation of complex morphological evolution over centuries, e.g. de Vriend *et al*. (1993), Bertin *et al*. (2009) and van der Wegen *et al*. (2010). Dissanayake *et al*. (2009) highlighted the influence of wave action on the channel equilibrium which is particularly important to the long-term inlet migration and ebb delta evolution. However, the accurate modelling of wave propagation over complex bathymetry and its interaction with tidal currents still remain a challenge. Furthermore, the stochastic nature of storm events makes it difficult to directly apply the morphological acceleration factor approach for a long-term forecasting under such complex conditions. Differences therefore have been found in many studies between modelled and observed ebb-tidal deltas. For example, van der Vegt *et al*. (2006) found that the modelled channels are deeper than observed ones and bending of the modelled ebb-tidal delta around the ebb channel can be under-estimated.

The present study focuses on the calibration of a two-dimensional, depth-averaged morphological model , which is setup to represent a large-scale laboratory experiment for a direct comparison without using a morphological factor. The model results highlight the importance of wave-current interaction, the intra-tidal transport variations and cross-shore transport on the morphology. The model also includes a novel approach to deal with the effects of side erosion to allow the effective evolution and migration of the inlet.

## NUMERICAL METHOD

The modelling system used in this study includes a wave propagation module, a depth-averaged current module, a sediment transport module and a morphological evolution module (Li *et al*. 2007). The wave module is based on energy and kinematic conservation equations for wave height and direction. It uses a set of intra-wave period equations (Yoo *et al* 1989) with modification proposed by Watanabe and Maruyama (1986). By solving the continuity and momentum equations, the instantaneous water surface and fluid volume fluxes can be found at each grid node. Wave height and propagation directions can be determined through integration over time at each node. Wave refraction, diffraction and reflection have been included in the solution without any special treatment. Wave breaking is dealt with through energy dissipation approach as suggested by Watanabe and Maruyama

[1] Centre for Engineering Sustainability, University of Liverpool, Brownlow Hill, Liverpool, L69 3GQ, United Kingdom.

[2] School of Engineering, Cardiff University, the Parade, Cardiff, CF24 3AA, United Kingdom.

(1986) for regular waves and Anastasiou and Bokaris (2000) for irregular waves. More details of the model can be found in Li *et al*. (2007), Fernando and Pan (2005) and O'Connor and Nicholson (1997).

Based on the computed wave characteristics, radiation stress terms can then be found and input into the depth-integrated flow module, which solves the depth-and-wave averaged continuity and momentum equations at each grid nodes, for calculating wave driven current:

$$\frac{\partial U}{\partial t}+\frac{\partial U^2}{\partial x}+\frac{\partial UV}{\partial y}+\frac{1}{\rho d}\left(\frac{\partial S_{xx}}{\partial x}+\frac{\partial S_{xy}}{\partial y}\right)+g\frac{\partial \eta}{\partial x}+\frac{\sqrt{U^2+V^2}}{d}C^uU-\frac{\partial}{\partial x}\left(\nu\frac{\partial U}{\partial x}\right)-\frac{\partial}{\partial y}\left(\nu\frac{\partial U}{\partial y}\right)=0 \quad (1)$$

$$\frac{\partial V}{\partial t}+\frac{\partial UV}{\partial x}+\frac{\partial V^2}{\partial y}+\frac{1}{\rho d}\left(\frac{\partial S_{yy}}{\partial y}+\frac{\partial S_{xy}}{\partial x}\right)+g\frac{\partial \eta}{\partial y}+\frac{\sqrt{U^2+V^2}}{d}C^vV-\frac{\partial}{\partial x}\left(\nu\frac{\partial V}{\partial x}\right)-\frac{\partial}{\partial y}\left(\nu\frac{\partial V}{\partial y}\right)=0 \quad (2)$$

$$\frac{\partial \eta}{\partial t}+\frac{\partial (Ud)}{\partial x}+\frac{\partial (Vd)}{\partial y}=0 \quad (3)$$

where U and V are depth-and-wave integrated flow velocities in x and y direction respectively, $S_{xx}$,, $S_{xy}$ and $S_{yy}$ are radiation stress tensor from wave action, $g$ is acceleration due to gravity, $\rho$ is fluid density, d is water depth, $C^v$ is friction factor, $\eta$ is water surface elevation and $\nu$ is turbulent viscosity. The friction factor for combined wave-current flow is computed based on Yoo et al (1989), and the mixing coefficient is determined by a two equation k-e closure as O'Connor et al (2000).

The sediment transport module computes the combined suspended load and bed load sediment fluxes. The suspended sediment transport rate is computed based on empirical expression for the potential load under combined waves and current (O'Connor and Nicholson 1997). The bed load transport rate is determined by the Einstein approach, as modified by O'Connor and Nicholson (1997). Then the bed level change can be computed by the sediment fluxes divergence equation, using a modified Lax-Wendroff scheme. The sediment flux divergence equation includes a gravitational term to allow for transport on slopes and takes the form as

$$\frac{\partial Z_B}{\partial t}=\frac{1}{\rho_s(1-n)}\left[-\frac{\partial}{\partial x}\left(Q_x-\alpha|Q_x|\frac{\partial Z_B}{\partial x}\right)-\frac{\partial}{\partial y}\left(Q_y-\beta|Q_y|\frac{\partial Z_B}{\partial y}\right)\right] \quad (4)$$

where $\rho_s$ is the sediment density, n is bed porosity, $Z_B$ is bed level, $Q_x$, $Q_y$ are the transport rate in x and y directions, $\alpha$ and $\beta$ are the slope parameters. To deal with the erosion of side slopes due to avalanching, the Chesher (1995) approach is employed:

$$Q_{xl}=CAV\left[\left(s^2+BU_{orb}{}^2\right)^{0.5}-U_{cr}\right]^{2.4}\frac{\partial Z_B}{\partial x} \quad (5)$$

$$Q_{yl}=CAU\left[\left(s^2+BU_{orb}{}^2\right)^{0.5}-U_{cr}\right]^{2.4}\frac{\partial Z_B}{\partial y} \quad (6)$$

where $Q_{xl}$, $Q_{yl}$ are the lateral flux in x and y direction respectively, C and A are model parameters, s is current speed, B is efficient factor, $U_{orb}$ is wave orbital speed and $U_{cr}$ is the critical velocity for sediment motion. More details of the above formulation can be found in Chesher (1995). Model results have suggested that the above formulations are particularly important to determine the position of up or down drift of the inlet breach correctly.

An explicit finite difference scheme is used to solve the equations on a regular C-type of grid. The x coordinate is defined for the long-shore direction and y coordinate for the cross-shore direction. The computed currents are then fed back to the wave module to determine the modified wave field due to currents, so the full interaction between hydrodynamics and morphodynamics is included.

## MODEL SETUP

The model was applied to the laboratory experiments carried out by Delft Hydraulics (1982) with a model of Keta Lagoon. In the laboratory experiments, the maximum offshore depth was 0.29m, the lagoon depth was 0.01m, both at mean water level, and the computational domain was represented by 100 and 74 cells in the longshore and cross-shore directions respectively, see Fig 1. The time step for the hydrodynamic calculations was set at 0.05s and that for the sediment transport and morphodymic

calculations was set at 5.0s. The tidal period was 2.5hr and the tidal range was 0.025m. Random waves with a significant height of 7cm and a peak period of 1.5s at 15° to the normal direction were used in the simulation. The sediment particle had a spatially uniform size of 0.21mm.The same conditions were used in the model simulations.

The model was calibrated against available laboratory data, including littoral sediment transport rate, mean inlet velocity and inlet sediment transport rate during both the ebb and flood tidal phases (Delft Hydraulics 1982). The model was then run for a total of 68 tidal cycles, each cycle consisting of a 1hr flood phase, a 1hr ebb phase and two 1/4hr transitional phases (see Fig 2), the same as used in the laboratory experiments.

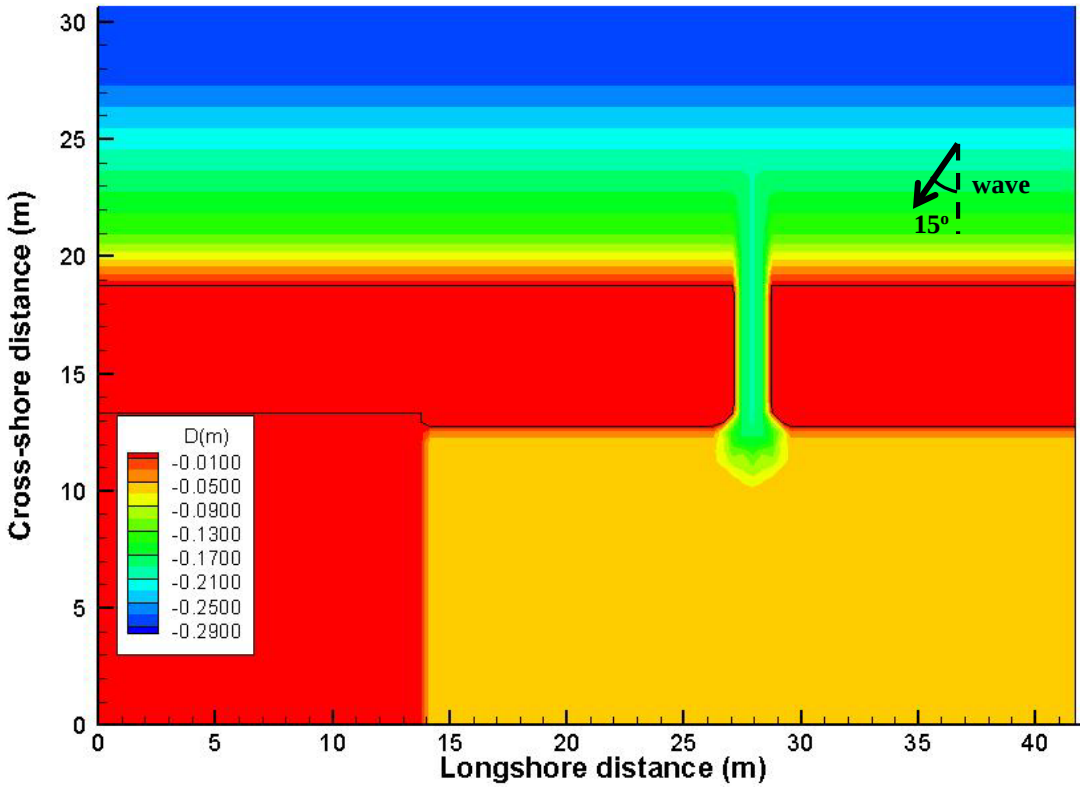


**Fig 1 Layout of the computational domain and initial bathymetry.**

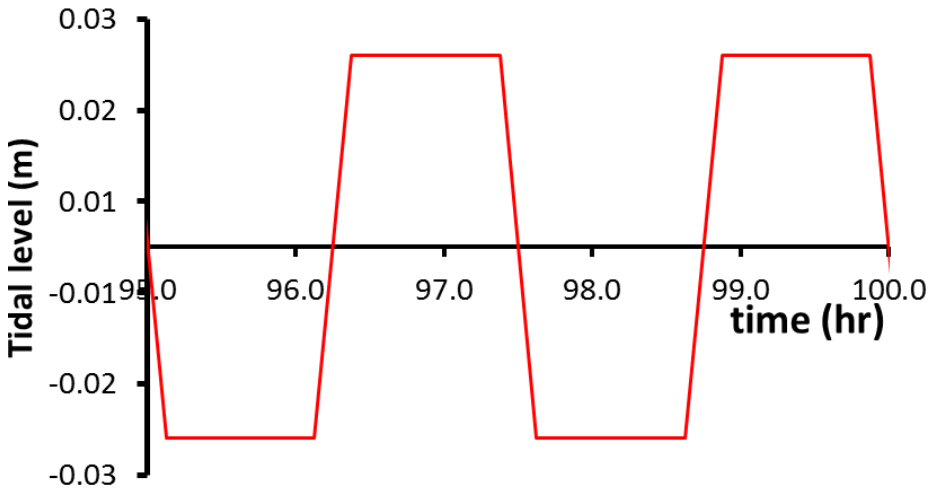


**Fig 2 Tidal level variation at the offshore boundary.**

## MODEL RESULTS

The computed variations of flow velocity and wave amplitude over a typical tidal period are presented in Fig 3. At the ebb, the strong jet of flow from lagoon towards the offshore area is clearly visible at the lagoon breach (inlet). Once reaches the outside the lagoon, the flow interacts with the longshore current and creates a large eddy at the downstream of the lagoon entrance. The increase in wave height at offshore side of the eddy is also noticeable, whereas waves can only penetrate into the seawards part of the inlet due the blockage caused by the flow in the inlet, and there are no waves inside the lagoon. At the flood, the tidal flow squeezes through the inlet and flushes inside the lagoon area. The longshore current at the offshore side of the lagoon is affected within a smaller area in comparison with that during the flood. The wave is able to penetrate to some distance in the inlet, leading to a slight increase in wave height there. At the offshore of the lagoon, the wave height slightly decreases at these circulations. During the course of simulation, with the changing in bathymetry, such flow patterns largely remains, but with a gradual downstream drifting of the inlet entrance.

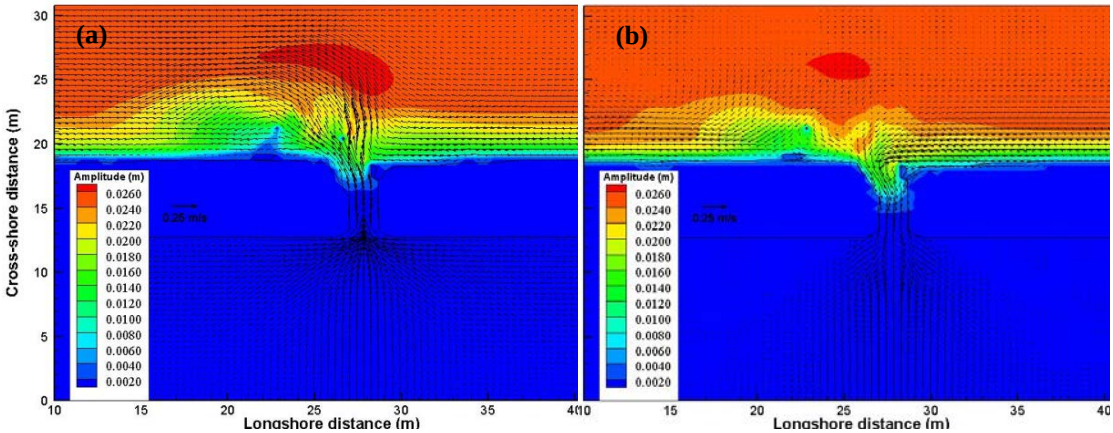


**Fig 3 Computed flow velocity vectors and wave amplitudes at ebb (a) and flood (b).**

Fig 4 presents the computed sediment transport vector and the corresponding bed level change at ebb and flood. The results shown in Fig 4 (a) and (b) represent the evolution at an earlier stage of the processes, while Fig 4 (c) and (d) show the bed level changes for a later stage of the change. It is clear that the overall pattern at the different stages are similar, i.e. at ebb, sediment transport is dominated by the longshore drift outside the lagoon with a clear erosion on the up drift of the inlet and the deepening of the channel; at flood, the longshore drift is interrupted by a cross-shore transport towards the lagoon entrance together with a reduced transport rate at the immediate up-drift of the breach. Through the time (68 tides), the offshore delta grows gradually in both ebb and flood phases. Similarly, the erosion at the down-drift of the breach is also clearly noticeable. The avalanching causes two effects, firstly it gradually widens up the breach entrance, which allows stronger exchange of flow and sediment across the lagoon gap. Secondly, the side slope erosion also reduces the width of the lagoon bank immediately upstream of the breach. The deposition near the up-drift of the breach entrance results in a down-drifting of the inlet as observed in many laboratory and field conditions. Inside the lagoon, however, changes are fairly small due to the reduced flow velocity with virtually no waves.

Fig 5 compares the computed and measured bed level changes after 68 tides. As expected, the major changes can be found around the inlet entrance where the flood flows erode the downstream the bank and the ebb flow deepens the channel in the middle. The deposition around the upstream of the breach entrance is largely due to the reduced longshore transport at the flood at this site (see Fig 4 b&d). The measured distribution of the evolution is fairly similar to the computed results in terms of both positions of erosion and deposition and their magnitudes. The differences largely lie in the deposition around the up-drift of the breach entrance, where the measured value is much larger than that from the model. In addition, the reduction in the bank width in the down-drift area of the entrance is also noticeable in the measurements, but not seen in the model predictions. This is partly due to the lack of cross-shore transport in the model, similar to most 2D depth averaged models in the literature.

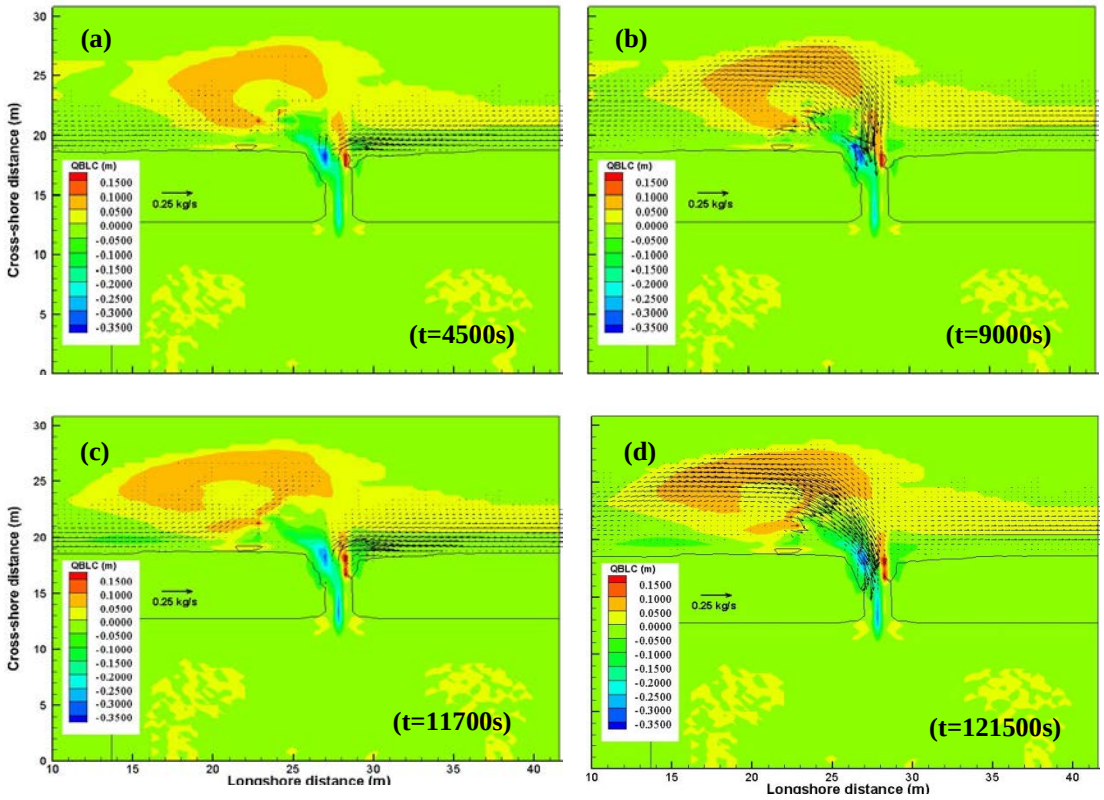


**Fig 4 Distribution of computed sediment transport vector and bed level change at ebb (a), (c) and flood (b) (d).**

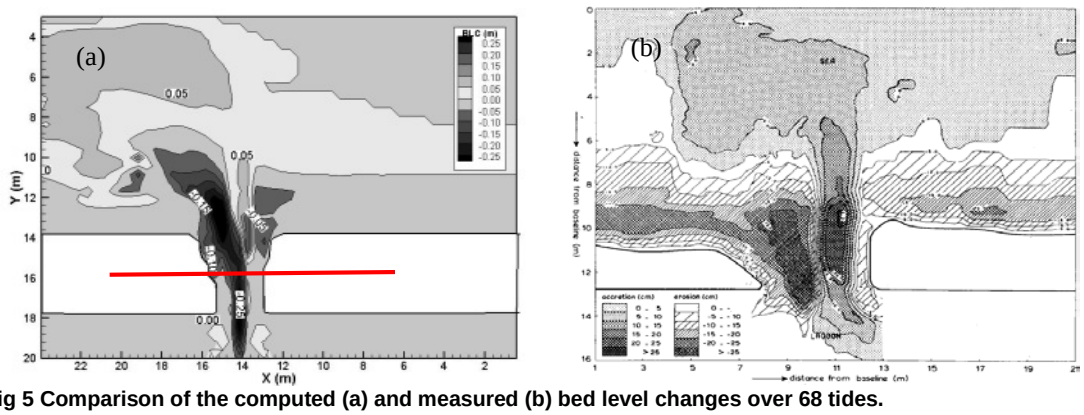


**Fig 5 Comparison of the computed (a) and measured (b) bed level changes over 68 tides.**

Fig 6 shows the comparison of the computed and measured bed level after 68 tidal cycles along the longshore direction (x) across the inlet, as shown in Fig 5(a). The solid line denotes the computed results and the symbols represent the measured values in the laboratory experiments. It can be seen that the predicted changes follows the measured data very well at the upstream of the gap where the deposition occurs. At the downstream of the gap, the erosion depth is under-predicted by the model and the gap width is narrower than that measured in the experiment. This is linked with fact that the down-drift seaward bank is not eroded in the model as much as measured in the laboratory experiments as shown in Fig 5: the measured data suggested a much stronger sidewall erosion of the downstream bank and hence led to a widening of the inlet as a result of reduced sediment supply at this site. Such a process is less well represented in this model study. However, the overall agreement can be regarded as acceptable as the main features in morphological changes are reasonably represented. The discrepancies may be also due to the uncertainties in the model parameters used for such a complex case, which are difficult to quantify.

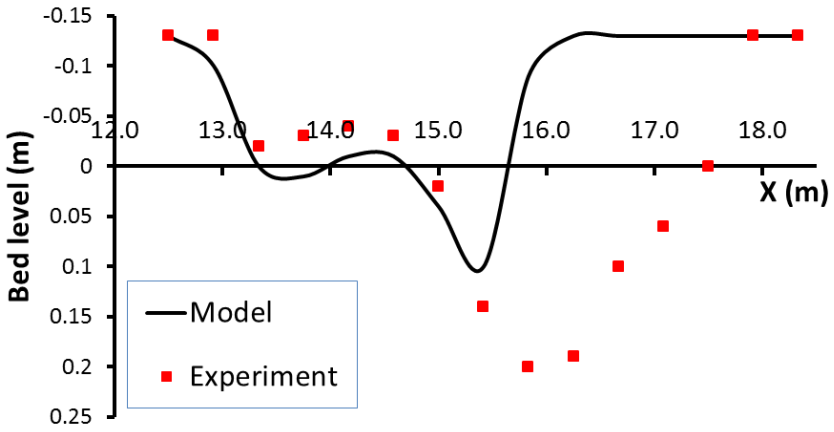


**Fig 6 Comparison of computed and measured bed level along the section indicated in Fig 5(a) after 68 tidal cycles.**

## CONCLUSIONS

The computed morphological changes clearly follow the measured data well. The results also reveal that the evolutions over the period of 68 tides are not uniformly: rapid and large accretion near the 'up-drift' of the inlet is apparent at the beginning of the simulation, and accelerative erosion near the 'down-drift' can be observed at late stages. This is largely due to the fact that at the flood phases, the sediment is transported into the lagoon, narrowing down the inlet width, while at the ebb phases, strong ebb flow erodes the bank and migrate the breach 'down-drift'. This effect becomes more significant at the later stages while the inlet becomes narrower and erosion accelerates as a result. However, it should be noted that the computer model used lacks capability of simulating the cross-shore sediment transport induced by waves, which has been observed in the laboratory experiments as the significant part of the berm being eroded over the test period. A full 3D model is currently used to investigate these effects.

## ACKNOWLEDGEMENT

This study was partly supported by the Engineering and Physical Sciences Research Council (UK) under grant EP/J005541/1(SINBAD) and EU MAST III INDIA project.

This paper is especially dedicated Dr John Nicholson, a co-author of this paper, who sadly passed away while this paper was written after an extraordinary battle against his illness. He had spent much his retirement in continuing his research on modelling coastal morphology, which formed part of this paper. He is dearly remembered.

## REFERENCES

Anastasiou, K. and Bokaris, J. (2000) Physical and numerical study of 2-D wave breaking and non-linear effects. Proceedings of the international Conference on Coastal Engineering, (Ed) Smith, J. M., Sydney, Australia, World Scientific, 382 – 395.

Bertin, X., Oliveira, A., Fortunato, A.B., 2009a. Simulating morphodynamics with unstructured grids: description and validation of a modeling system for coastal applications. Ocean Modelling 28 (1–3), 75–87.

Bruun, P., Mehta, A.J., Johnsson, I.G., 1978. Stability of Tidal Inlets. Theory and Engineering, Elsevier Scientific, Amsterdam, The Netherlands, p. 506.

Chester, T. (1995) Numerical morphodynamic modelling of Keta Lagoon, in Dally, W. and Zeidler R. (Ed) Proceedings of the International Conference on Coastal Research in Terms of Large Scale Experiments, Portland, ASCE, New York.

Davis, R.A., Barnard, P., 2003. Morphodynamics of the barrier–inlet system, westcentral Florida. Marine Geology 200 (2003), 77–101.

De Vriend, H.J., Capobianco, M., Chesher, T., de Swart, H.E., Latteux, B., Stive, M.J.F., 1993. Approaches to long-term modelling of coastal morphology: a review. Coastal Engineering 21 (1–3), 225–269.

Delft Hydraulics (1982) Outfall Keta Lagoon, Report M 1613, 63pp.

Fernando, P. T. and Pan S. (2005) Modelling wave of hydrodynamics around a scheme of detached leaky breakwaters, Proceeding of the 29th International conference on Coastal Engineering, (Ed) Smith, J. M., Lisbon, Portugal, World Scientific, 830-841.

Hayes, M.O., 1979. Barrier Island morphology as a function of tidal and wave regime. In: Leatherman (Ed.), Barrier Island. Academic Press, New York, pp. 1–28.

Hayes, M.O., 1980. General morphology and sediment patterns in tidal inlets. Sedimentary Geology, vol. 26. Elsevier, Amsterdam, pp. 139–156.

Dissanayake, D., Roelvink, J. and van der Wegen M. (2009) Modelled channel patterns in a schematized tidal inlet, Coastal Engineering (56), 1069-1083

Li, M., Fernando, P., Pan, S., O'Connor, B.A., Chen, D. (2007) Development of a quasi-3d numerical model for sediment transport prediction in the coastal region, Journal of Hydro-environment Research (1), 143-156.

O'Connor, B. A., Pan, S., Heron, M., Williams, J., Voulgaris, G., and Silva, A. (2000) Hydrodynamic modelling of a dynamic inlet, Proceedings of the International Conference on Coastal Engineering, (Ed) Smith, J. M., Sydney, Australia, World Scientific, 3472-3481.

O'Connor, B.A. and Nicholson, J. 1997. Tidal sediment transport. In: Acinas, J.R. and Brebbia, C.A. (Editors), Computer Modelling of Seas and Coastal Regions III, Computational Mechanics Publications, 367-379.

Van Der Wegen, M., Dastgheib, A., Roelvink, J.A., 2010. Morphodynamic modelling of tidal channel evolution in comparison to empirical PA relationship. Coastal Engineering 57, 827–837.

Van Der Vegt, M., Schuttelaars, H.M., De Swart, H.E., 2006. Modelling the equilibrium of tide-dominated ebb-tidal deltas. Journal of Geophysical Research 111, F02013.

Watanabe, A. and Maruyama, K (1986) Numerical modelling of nearshore wave field under combined refraction, diffraction and breaking, Coastal Engineering in Japan, 29, 19-39.

Yoo, D., Hedges, T. and O'Connor B. A. (1989) Numerical modelling of reflective waves on slowly varying currents, Advances in water modelling and measurements (Ed) Palmer, M.H., 297-306.